Version: Pre-print

Asymptotic Pairwise Dispersion Corrections Can Describe Layered Materials Accurately

A. Otero-de-la-Roza,*,† Luc M. LeBlanc,*,‡ and Erin R. Johnson*,‡

Departamento de Química Física y Analítica, Facultad de Química, Universidad de Oviedo, 33006 Oviedo, Spain, and Department of Chemistry, Dalhousie University, 6274 Coburg Rd, Halifax, Nova Scotia, B3H 4R2, Canada

E-mail: aoterodelaroza@gmail.com; luc.leblanc@dal.ca; erin.johnson@dal.ca

Abstract

A recent study by Tawfik et al. [*Phys. Rev. Mater.*, **2** (2018) 034005] found that few density functionals, none of which are asymptotic pairwise dispersion methods, describe the geometry and binding of layered materials accurately. Here, we show that the exchange-hole dipole moment (XDM) dispersion model attains excellent results for graphite, hexagonal BN, and transition-metal dichalcogenides. Contrary to what has been argued, succesful modeling of layered materials does not necessitate meta-GGA exchange, non-local correlation functionals, or the inclusion of three-body dispersion terms. Rather, a GGA functional, combined with a simple asymptotic pairwise dispersion correction, can be reliably used provided that it properly accounts for the geometric dependence of the dispersion coefficients. The overwhelming contribution to the variation of the pairwise dispersion coefficients comes from the immediate vicinity of an atom, and is already present for single layers, although longer-range effects must also be captured in delocalized systems, such as graphite.

Layered materials consist of aggregates of two-dimensional sheets, with strong in-plane and weak out-of-plane interactions. The interest in layered materials arises from their ex- otic electronic properties and easy exfoliation, which allows manufacturing atomically thin single layers, or stacks of these layers, with potential technological applications.[1] These materials have received much recent attention due to their desirable properties for superlubricity,[2] photodetectors,[3] optical modulators,[4] non-linear optics,[5] and other optoelectronics applications.[6]

Because of the weak van der Waals nature of interlayer binding, layered materials have served as stringent tests to assess the performance of various computational methods for the description of London dispersion.[7–10] Within density-functional theory (DFT), a large number of dispersion corrections and dispersion-including functionals,[11–14] with varying degrees of empiricism, are now available. Some of these methods are highly successful for interactions between organic molecules (e.g. the DFT-D family of dispersion corrections[15–17]), while others are more suited to the description of condensed materials (e.g. the vdw-DF non-local functionals[18,19]). Ideally, it would be desirable to have dispersion-corrected functionals that are able to treat all kinds of systems on an equal footing.[14]

There are significant differences in the quality of various dispersion-corrected DFT methods for inorganic applications, such as surface adsorption[20] and, particular to the focus of this work, layered materials.[8–10] Tawfik et al.[10] and Björkman et al.[9,21] performed exten-

---

*To whom correspondence should be addressed
†Universidad de Oviedo
‡Dalhousie University

sive benchmark tests on different dispersion-corrected functionals for simple layered systems. According to their results, asymptotic pairwise dispersion methods, and most non-local dispersion functionals, are not able to provide a reasonable treatment of both the binding energies and interlayer separations simultaneously.[10] Good performance for one quantity tends to be offset by large errors for the other. Only the fractionally-ionic (FIA) variant[22] of the many-body dispersion[23] (MBD) model, the SCAN functional coupled with non-local rVV10 dispersion,[24] and some non-local vdw-DF functionals[9] have been shown to give consistently accurate performance for both geometry and energetics. Tawfik et al. conclude that "meta-GGAs may offer a superior starting point for dispersion corrections" and propose combining meta-GGAs with dispersion corrections such as FIA for better performance.[10] This is an undesirable state of affairs because the practical application of these methods is hampered by poor scaling with system size, computational complexity (non-local functionals with meta-GGA exchange), and convergence difficulties (MBD), and also because their wider applicability to other types of systems is unclear. In this letter, we argue that a simple GGA with an asymptotic pairwise dispersion correction can described layered materials accurately, provided it captures the non-additivity of the pairwise coefficients correctly.

Asymptotic pairwise dispersion corrections are both simple to calculate and accurate for interactions between organic molecules. However, there are open questions concerning the importance of non-additivity in the pairwise coefficients and arising from atomic many-body terms, the leading-order being the Axilrod-Teller-Muto (ATM)[25,26] three-body contribution.[10] In this letter, we attempt to answer these questions by analyzing the performance of the exchange-hole dipole moment (XDM) dispersion model[14,27,28] for layered materials. XDM is an asymptotic pairwise dispersion correction that has demonstrated excellent performance for systems typically studied in gas-phase chemistry,[29] as well as for molecular crystals,[14,30] metal surfaces,[20] and graphene ad-

sorption.[31,32] The XDM dispersion coefficients are non-empirical, semilocal functions of the electron density, its derivatives, and the kinetic energy density, and therefore include electronic many-body effects to all orders through use of a fully self-consistent set of Kohn-Sham states.

For comparison with previous literature, we consider both the same benchmark set of 11 layered materials studied by Tawfik and co-workers[10] (graphite, h-BN, MoS_2, $MoSe_2$, $MoTe_2$, WS_2, TaS_2, HfS_2, $HfSe_2$, $HfTe_2$, and $PdTe_2$) and the full set of 26 layered materials proposed by Björkman et al.[9,21] All calculations were carried out with the Quantum ESPRESSO program[33] using the projector-augmented wave (PAW) approach.[34] For consistency, the PBE functional[35] was used for calculations performed with the D2,[15] D3,[16] D3BJ,[36] and XDM[14,28] dispersion corrections. Additional calculations were also performed with B86bPBE,[35,37] which is the recommended functional for use with XDM in solid-state calculations.[14] MBD[23] calculations were also performed using the CASTEP program[38] with ultrasoft pseudopotentials for graphite to investigate the variation in dispersion coefficients with interlayer separation. However, MBD calculations could not be converged for the transition-metal dichalcogenides, in agreement with previous reports.[10] Further details regarding computational methods and reference data are given in the Supporting Information (SI).

Figure 1 shows the mean absolute errors in the lattice parameters and exfoliation energies obtained for Tawfik's subset of 11 layered materials.[10] Data reported[9,10] for several other dispersion-corrected DFT methods are also given for comparison. Full tables for both this subset, and for Björkman's full set of 26 layered materials, are given in the SI. To put the errors in context, the exfoliation energies range from 16.1 eV/Å^2 for HfS_2 to 40.2 eV/Å^2 for $PdTe_2$, with an average value of 20.3 meV/Å^2.

In agreement with Tawfik et al.,[10] most asymptotic pairwise dispersion corrections (D2, D3(0), D3(BJ), TS, and SCS-TS in Figure 1) give reasonable geometries, but significantly overestimate exfoliation energies. Conversely, some non-local vdW-DF methods and PBE-

Figure 1: Distribution of errors obtained with various dispersion-corrected DFT methods (only the optPBE result reported by Tawfik et al.[10] is shown). The shaded box represents an acceptable margin of error (5 meV/Å^2 and 0.2 Å).
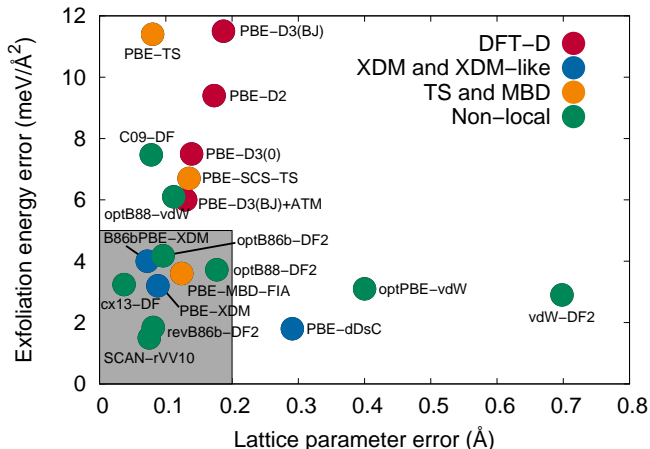
dDsC give reasonable exfoliation energies, but substantially overestimate the interlayer separations. PBE-MBD-FIA, SCAN-rVV10, and several non-local vdw-DF correlation plus purposely fitted exchange functionals were found to give accurate predictions of both geometries and energies for the benchmark systems. Among the pairwise dispersion correction methods, only XDM (in combination with either PBE or B86bPBE) yields accurate interlayer separations and exfoliation energies.

Focussing on the pairwise dispersion corrections, all members of the DFT-D family significantly overestimate the exfoliation energies. PBE-D3(BJ) results in worse exfoliation energies than the older PBE-D2, but the performance depends on which damping function is used. PBE-TS, according to Tawfik et al.,[10] overestimates the exfoliation energy nearly as much as PBE-D3(BJ). Inclusion of the three-body ATM term improves the PBE-D3(BJ) results, but the overestimation of the exfoliation energies is still present. This could be interpreted as an argument for the inclusion of the three-body ATM term. However, it is important to note that neither XDM, nor SCAN-rVV10, nor any of the other non-local functionals in the "good quality" zone of Figure 1, include three-body ATM dispersion terms (although it is possible to calculate the corresponding dispersion coefficients within XDM[39]). This suggests that a more likely explanation for the ATM term improving the performance of PBE-D3(BJ) is that it almost always gives a repulsive contribution, and the exfoliation energies predicted by PBE-D3(BJ) are severely overestimated.

While three-body dispersion effects are physical, Jankiewicz et al.[40] recently showed that most dispersion-corrected functionals, including the MBD method, fail to predict reasonable three-body interaction energies. The ATM term seems to mainly correct for other errors, such as the incorrect dependence of the pairwise dispersion coefficients on chemical environment, missing higher-order pairwise terms (shown to lead to overbinding[39]), or errors from the base density functional. Indeed, in molecular systems, differences between the three-body interaction energies obtained with different base functionals are larger than the three-body dispersion energy itself.[11,41]

Additional calculations were carried out for the full set of 26 layered materials studied by Björkman[9,21] (see SI). Again, the B86bPBE-XDM and PBE-XDM functionals are the only asymptotic pairwise dispersion methods that fall within the "good quality" zone of 0.2 Å and 5 meV/Å^2 error for interlayer lattice paremeters and exfoliation energies, respectively. Therefore, we conclude that XDM in its canonical pairwise form can be added to the small set of density-functional dispersion methods that perform reliably for layered materials.

To try to explain the large differences between asymptotic pairwise dispersion corrections, we turn to the analysis of the dispersion coefficients. Dobson recently classified various non-additive contributions to the dispersion energy into three categories (A, B, and C).[42] The Dobson-A contribution corresponds to the non-additivity caused by the variation in dispersion coefficients with the immediate environment of an atom. Dobson-B refers to non-pairwise dispersion energy terms, of which the leading-order is the ATM contribution. Dobson-C arises in the interaction between extended conducting systems at the infinite-separation limit

and is unlikely to be important here.[10]

The good performance of SCAN+rVV10[24] and several other non-local dispersion functionals[9] that do not include Dobson-B effects,[10,42] support the idea that Dobson-B effects seem not to be a requirement for good performance of a dispersion-corrected functional. We now consider Dobson-A, i.e., the change in atomic pairwise dispersion coefficients with the system's geometry, by focusing on the leading-order, C_6, dispersion coefficients. We note that, unlike TS, XDM is sensitive to many-body effects through changes in the exchange-hole dipole moment integrals and, therefore, our analysis of the non-additivity in the C_6 is not limited to the immediate vicinity of an atom.

We consider pairwise non-additivity in two steps: first, we analyze the change when going from a free atom to a single layer, and then from a single layer to the layered material. The average homoatomic C_6 dispersion coefficients for each element in the layered-materials benchmark obtained with D2, D3, and XDM are collected in Table 1, and compared to the free-atom reference value. XDM predicts large changes in homoatomic C_6 for the layered materials relative to the free atoms, which stem primarily from decreases in the exchange-hole dipole moment integrals, and cannot be captured by a simple scaling of the coefficients with the atomic volume. Similar behaviour was observed previously for metal surfaces and in bulk metals.[14,20,32]

While the D2 method uses fixed (empirical) atomic dispersion coefficients, and is pairwise additive by design, the more sophisticated D3 method employs dispersion coefficients that vary with coordination number and hence include some non-addivity. The reduction in C_6 for the layered materials seen with XDM is partially captured by D3, with the homoatomic C_6's for the transition metals being in fairly good agreement. However, the D3 C_6's are roughly twice the XDM values for the chalcogen atoms. The chalcogens lie at the edges of the 2D layers and most-closely approach their neighbours from the adjacent layers, perhaps explaining the systematic overbinding seen with D3. The results suggest that, while the *ad hoc*

Table 1: Average homoatomic C_6 dispersion coefficients (in atomic units) used for the Tawfik subset of 11 layered materials with selected dispersion methods.

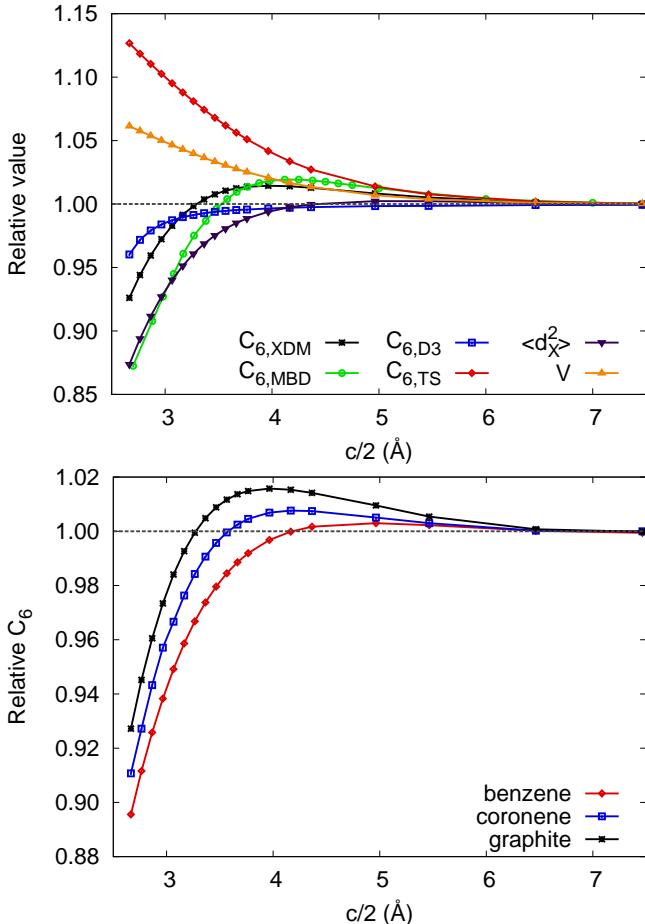| Atom	Free[a]	D2[b]	D3[c]	XDM[c,d,e]
B	99.5	54.29	31.45	29.43
C	46.6	30.35	24.28	17.98
N	24.2	21.33	15.61	11.69
S	134.0	96.61	125.8	64.01
Se	210.0	219.2	210.5	98.01
Te	396.0	550.6	418.6	175.7
Mo	1029	427.9	337.1	365.8
Pd	157.5	427.9	265.9	112.9
Hf	1275	1409	421.0	562.8
Ta	1020	1409	458.8	399.7
W	847.9	1409	398.1	307.9

[a]The reference free-atom dispersion coefficients employed in the TS model. [b]The D2 values are constant for each element. [c]Values in the limit of large interlayer separations are reported. [d]Results use PBE densities, although they are effectively identical with B86bPBE. [e]Values correspond to the average over all materials sharing a given element.

formulas used in the calculation of the D3 coefficients work very well for non-covalent interactions between organic molecules, they may not be adequate for more exotic systems, such as transition metal chalcogenides, due to an incorrect treatment of non-additivity in the pairwise coefficients.

Now we examine the variation in dispersion coefficients due to the presence of neighbouring layers within the materials. We focus on graphite, since the C_6 is identical for all atoms within the unit cell and also because MBD calculations can be performed for the purpose of comparison. The TS coefficients are calculated by scaling the reference C_6 for carbon (32.89 a.u.) with the Hirshfeld volumes calculated in XDM.

The relative change in C_6 with interlayer separation is shown in Figure 2 (top) for the D3, TS, XDM, and MBD dispersion models. The D3 dispersion coefficient depends only on the coordination number, and its value decreases smoothly with interlayer separation as the co-

Figure 2: Change in C_6 dispersion coefficients with interlayer separation in graphite (top) and with layer type (bottom). In the upper plot, changes in the dipole-moment integrals, $\langle d_X^2 \rangle$, and atomic volumes, V, are also shown. Values are expressed relative to those obtained in the limit of large interlayer separation.

the atomic volumes,[44] they increase even more steeply with decreasing interlayer separation. This behaviour of TS is opposite to all other dispersion corrections and, importantly, to its successor, the MBD method.

The XDM and MBD dispersion models have a more sophisticated dependence on chemical environment, fully accounting for effects of neighbouring atoms on the electron density distribution and C_6. The results of these models for graphite are in striking agreement, particularly considering how different the two dispersion models are. Both predict an initial rise in C_6 on compression, followed by a sharp decrease at small interlayer separations. In XDM, this can be explained by the interplay between volume (or polarizability), which provides the initial rise in C_6, and the exchange-hole dipole moment integral, which leads to a rapid decrease in C_6 at small separations. From the graphite example, it is clear that XDM and MBD are capturing the same effects regarding non-additivity of the pairwise term (referred to as many-body effects in the MBD literature[12,45]).

In the Dobson classification, it is assumed that Dobson-A non-additivity comes exclusively from the local environment of an atom.[42] To test this, we examined the variation in the carbon C_6 with exfoliation in graphite and compared it to the same interlayer geometries but with graphene layers replaced with benzene and coronene molecules (Figure 2, bottom). There are significant differences in C_6 variation in these three cases, indicating that there is a significant contribution to non-additivity from distant atoms within the same or opposing layers. Combined with previous findings regarding the large variation of the exchange-hole dipole moment integrals for bulk metals and surfaces,[20,32] and the high non-locality of the exchange-hole in graphite,[46] our observations strongly suggest that interatomic delocalization plays a fundamental role in pairwise non-additivity.

To summarize, layered systems are an extremely sensitive benchmark for density-functional dispersion methods. In agreement with Tawfik et al., we found no evidence that the inclusion of three-body ATM terms is necessary for modeling layered materials accurately.

ordination number decreases, with the slope becoming steeper at shorter distances. In contrast, the integrated atomic volume, used in the evaluation of the TS and XDM dispersion coefficients, increases at shorter distances. While an increase in atomic volume with compression is counterintuitive, this can be explained by the use of Hirshfeld partitioning and the way volumes are calculated.[43] As the layers are compressed, the region of space where the corresponding Hirshfeld weights are significant is reduced but, at the same time, the density tails from adjacent layers contribute to the volume integrals, which results in an overall increase in atomic volume. As the TS dispersion coefficients are proportional to the square of

However, we demonstrated that, contrary to previous works,[9,10] a GGA plus an asymptotic pairwise dispersion correction can be highly accurate for layered materials, provided pairwise non-additivity is captured correctly. Specifically, XDM gives similar performance to much more computationally complex methods, such as the non-pairwise PBE-MBD-FIA and the non-local meta-GGA SCAN-rVV10, for inter-layer separations. Our study of graphite indicates that the dependence of the XDM dispersion coefficients on the system geometry is similar to that of MBD (although MBD calculations cannot be applied to transition metal dichalcogenides without modification[22] because the calculations do not converge[10]), and that there is significant pairwise non-additivity, primarily arising from variations in the electron distribution within a single atomic layer.

XDM retains all the advantages of a pairwise dispersion correction, namely, a simple implementation, low scaling with system size, and negligible computational cost. No modification or reparametrization of XDM was needed and the exact same methodology also excels for organic molecules,[14,29] molecular crystals,[14,30] metal surfaces,[20] and graphene adsorption,[31,32] enabling the use of XDM-corrected functionals for modeling complex chemistry in layered materials.

Supporting Information Available: Additional method details; discussion of interlayer non-additivity effects; unit-cell images; calculated and reference inter-layer lattice parameters and exfoliation energies; tables of absolute and percent errors. This material is available free of charge via the Internet at http://pubs.acs.org/.

References

(1) Geim, A. K.; Grigorieva, I. V. Van der Waals heterostructures. *Nature* **2013**, *499*, 419.

(2) Berman, D.; Erdemir, A.; Sumant, A. V. Approaches for Achieving Superlubricity in Two-Dimensional Materials. *ACS Nano* **2018**, *12*, 2122–2137.

(3) Xie, C.; Mak, C.; Tao, X. M.; Yan, F. Photodetectors Based on Two-Dimensional Layered Materials Beyond Graphene. *Adv. Funct. Mater.* **2017**, *27*, 1603886.

(4) Sun, Z. P.; Martinez, A.; Wang, F. Optical modulators with 2D layered materials. *Nat. Photonics* **2016**, *10*, 227–238.

(5) Autere, A.; Jussila, H.; Dai, Y. Y.; Wang, Y. D.; Lipsanen, H.; Sun, Z. P. Nonlinear Optics with 2D Layered Materials. *Adv. Mater.* **2018**, *30*, 1705963.

(6) Zhou, X.; Hu, X. Z.; Yu, J.; Liu, S. Y.; Shu, Z. W.; Zhang, Q.; Li, H. Q.; Ma, Y.; Xu, H.; Zhai, T. Y. 2D Layered Material-Based van der Waals Heterostructures for Optoelectronics. *Adv. Funct. Mater.* **2018**, *28*, 1706587.

(7) London, F. On the theory and systematic of molecular forces. *Z. Physik* **1930**, *63*, 245–279.

(8) Björkman, T.; Gulans, A.; Krasheninnikov, A. V.; Nieminen, R. M. Are we van der Waals ready? *J. Phys.: Condens. Matter* **2012**, *24*, 424218.

(9) Björkman, T. Testing several recent van der Waals density functionals for layered structures. *J. Chem. Phys.* **2014**, *141*, 074708.

(10) Tawfik, S. A.; Gould, T.; Stampfl, C.; Ford, M. J. Evaluation of van der Waals density functionals for layered materials. *Phys. Rev. Mater.* **2018**, *2*, 034005.

(11) Grimme, S.; Hansen, A.; Brandenburg, J. G.; Bannwarth, C. Dispersion-Corrected Mean-Field Electronic Structure Methods. *Chem. Rev.* **2016**, *116*, 5105–5154.

(12) Hermann, J.; DiStasio Jr., R. A.; Tkatchenko, A. First-Principles Models for van der Waals Interactions in Molecules and Materials: Concepts, Theory, and Applications. *Chem. Rev.* **2017**, *117*, 4714–4758.

(13) DiLabio, G. A.; Otero-de-la-Roza, A. In *Reviews in Computational Chemistry*; Lipkowitz, K. B., Ed.; Wiley-VCH, 2016; Vol. 29; pp 1–97.

(14) Johnson, E. R. In *Non-covalent Interactions in Quantum Chemistry and Physics*; Otero-de-la-Roza, A., DiLabio, G. A., Eds.; Elsevier, 2017; Chapter 5, pp 169–194.

(15) Grimme, S. Semiempirical GGA-type density functional constructed with a long-range dispersion correction. *J. Comput. Chem.* **2006**, *27*, 1787–1799.

(16) Grimme, S.; Antony, J.; Ehrlich, S.; Krieg, H. A consistent and accurate ab initio parametrization of density functional dispersion correction (DFT-D) for the 94 elements H-Pu. *J. Chem. Phys.* **2010**, *132*, 154104.

(17) Caldeweyher, E.; Bannwarth, C.; Grimme, S. Extension of the D3 Dispersion Coefficient Model. *J. Chem. Phys.* **2017**, *147*, 034112.

(18) Dion, M.; Rydberg, H.; Schröder, E.; Langreth, D. C.; Lundqvist, B. I. Van der Waals density functional for general geometries. *Phys. Rev. Lett.* **2004**, *92*, 246401.

(19) Lee, K.; Murray, É. D.; Kong, L.; Lundqvist, B. I.; Langreth, D. C. Higher-accuracy van der Waals density functional. *Phys. Rev. B* **2010**, *82*, 081101.

(20) Christian, M. S.; Otero-de-la-Roza, A.; Johnson, E. R. Surface adsorption from the exchange-hole dipole moment dispersion model. *J. Chem. Theory Comput.* **2016**, *12*, 3305.

(21) Björkman, T.; Gulans, A.; Krasheninnikov, A.; Nieminen, R. van der Waals Bonding in Layered Compounds from Advanced Density-Functional First-Principles Calculations. *Phys. Rev. Lett.* **2012**, *108*, 235502.

(22) Gould, T.; Lebègue, S.; Ángyán, J. G.; Bučko, T. A Fractionally Ionic Approach to Polarizability and van der Waals Many-Body Dispersion Calculations. *J. Chem. Theory Comput.* **2016**, *12*, 5920–5930.

(23) Tkatchenko, A.; DiStasio, R. A.; Car, R.; Scheffler, M. Accurate and Efficient Method for Many-Body van der Waals Interactions. *Phys. Rev. Lett.* **2012**, *108*, 236402.

(24) Peng, H.; Yang, Z.-H.; Perdew, J. P.; Sun, J. Versatile van der Waals Density Functional Based on a Meta-Generalized Gradient Approximation. *Phys. Rev. X* **2016**, *6*, 041005.

(25) Axilrod, B. M.; Teller, E. Interaction of the van der Waals type between three atoms. *J. Chem. Phys.* **1943**, *11*, 299–300.

(26) Muto, Y. *J. Phys. Math. Soc. Japan* **1943**, *17*, 629.

(27) Becke, A. D.; Johnson, E. R. Exchange-hole dipole moment and the dispersion interaction revisited. *J. Chem. Phys.* **2007**, *127*, 154108.

(28) Otero-de-la-Roza, A.; Johnson, E. R. Van der Waals interactions in solids using the exchange-hole dipole moment. *J. Chem. Phys.* **2012**, *136*, 174109.

(29) Otero-de-la-Roza, A.; Johnson, E. R. Non-Covalent Interactions and Thermochemistry using XDM-Corrected Hybrid and Range-Separated Hybrid Density Functionals. *J. Chem. Phys.* **2013**, *138*, 204109.

(30) Otero-de-la-Roza, A.; Cao, B. H.; Price, I. K.; Hein, J. E.; Johnson, E. R. Predicting the Relative Solubilities of Racemic and Enantiopure Crystals by Density-Functional Theory. *Angew. Chem. Int. Ed.* **2014**, *53*, 7879–7882.

(31) Christian, M. S.; Otero-de-la-Roza, A.; Johnson, E. R. Adsorption of graphene to metal (111) surfaces using the exchange-hole dipole moment model. *Carbon* **2017**, *124*, 531–540.

(32) Christian, M. S.; Otero-de-la-Roza, A.; Johnson, E. R. Adsorption of graphene to nickel (111) using the exchange-hole dipole moment model. *Carbon* **2017**, *118*, 184–191.

(33) Giannozzi, P. et al. Advanced capabilities for materials modelling with Quantum ESPRESSO. *J. Phys.: Condens. Matter* **2017**, *29*, 465901.

(34) Blöchl, P. E. Projector augmented-wave method. *Phys. Rev. B* **1994**, *50*, 17953.

(35) Perdew, J.; Burke, K.; Ernzerhof, M. Generalized gradient approximation made simple. *Phys. Rev. Lett.* **1996**, *77*, 3865–3868.

(36) Grimme, S.; Ehrlich, S.; Goerigk, L. Effect of the damping function in dispersion corrected density functional theory. *J. Comput. Chem.* **2011**, *32*, 1456–1465.

(37) Becke, A. D. On the large-gradient behavior of the density functional exchange energy. *J. Chem. Phys.* **1986**, *85*, 7184.

(38) Clark, S. J.; Segall, M. D.; Pickard, C. J.; Hasnip, P. J.; Probert, M. J.; Refson, K.; Payne, M. C. First principles methods using CASTEP. *Z. Kristallogr.* **2005**, *220*, 567–570.

(39) Otero-de-la-Roza, A.; Johnson, E. R. Many-body dispersion interactions from the exchange-hole dipole moment model. *J. Chem. Phys.* **2013**, *138*, 054103.

(40) Jankiewicz, W.; Podeszwa, R.; Witek, H. A. Dispersion-corrected dft struggles with predicting three-body interaction energies. *Journal of chemical theory and computation* **2018**, *14*, 5079–5089.

(41) Řezác, J.; Huang, Y.; Hobza, P.; Beran, G. J. O. Benchmark Calculations of Three-Body Intermolecular Interactions and the Performance of Low-Cost Electronic Structure Methods. *J. Chem. Theory Comput.* **2015**, *11*, 3065–3079.

(42) Dobson, J. F. Beyond pairwise additivity in London dispersion interactions. *Int. J. Quantum Chem.* **2014**, *114*, 1157–1161.

(43) Hirshfeld, F. L. Bonded-atom fragments for describing molecular charge densities. *Theor. Chim. Acta* **1977**, *44*, 129–138.

(44) Tkatchenko, A.; Scheffler, M. Accurate molecular van der Waals interactions from ground-state electron density and free-atom reference data. *Phys. Rev. Lett.* **2009**, *102*, 073005.

(45) DiStasio, R. A.; Gobre, V. V.; Tkatchenko, A. Many-body van der Waals interactions in molecules and condensed matter. *J. Phys.: Condens. Matter* **2014**, *26*, 213202.

(46) Otero-de-la-Roza, A.; Pendás, A. M.; Johnson, E. R. Quantitative electron delocalization in solids from maximally localized Wannier functions. *J. Chem. Theory Comput.* **2018**, *14*, 4699–4710.

Graphical TOC Entry